

**PERFORMANCE COMPARISON OF A-SI,  $\mu$ A-SI, C-SI AS A FUNCTION OF AIR MASS AND TURBIDITY**

Stefan Krauter<sup>1,2,3</sup> and Alexander Preiss<sup>1,2</sup>

<sup>1</sup>Photovoltaik Institut Berlin AG, Wrangelstr. 100, D-10977 Berlin, Germany  
 Phone: +49 (30) 814 52 64 0, Fax: +49 (30) 814 52 64 101, e-mail: preiss@pi-berlin.com

<sup>2</sup>Technical University Berlin, Sec. EM 4, Einsteinufer 11, D-10587 Berlin, Germany

<sup>3</sup>University of Paderborn, Faculty for Electrical Engineering, Informatics and Mathematics, Institute for Sustainable Energy Concepts, Pohlweg 55, D-33098 Paderborn, Germany, e-mail: krauter@nek.upb.de

**ABSTRACT:** Three different cell technologies have been compared in terms of  $I_{sc}$  and energy yield: c-Si, tandem  $\mu$ a-Si, and a-Si. Spectral and weak-light effects, degradation and regeneration have been investigated via on outdoor measurements in Berlin over one year; additionally weak-light performance using a sun-simulator has been examined. For high AM values performance of a-Si and  $\mu$ a-Si is reduced compared to c-Si, especially for clear sky conditions (up to 25%). This effect cannot be attributed to weak light effects, while weak light performance of the thin film technologies examined shown a weak light performance superior to that of c-Si used for reference. Over one year a slight increase of 2% for a-Si and  $\mu$ a-Si vs. c-Si has been observed in Berlin, Germany. As temperature coefficients for power output are lower than for c-Si technologies, yield increase might be even better under tropical conditions, also due to lower AMs and higher turbidity.

**Keywords:** yield, spectral effect, weak-light performance, degradation

**1 INTRODUCTION**

Accurate determination of power output and energy yield is crucial for profitable operation of PV power plants. While performance of c-Si based modules is well understood and implemented in state-of-the-art simulation programs, thin-film technologies such as a-Si and  $\mu$ -Si or tandem structures consisting of  $\mu$ -Si and a-Si based modules provide difficulties in performance determination, even after termination of the degradation process.

**1.1 Spectral effect**

Due to the different spectral responses of the PV technologies and their different matching to the actual solar spectrum, actual performance may change, as illustrated in Fig.1. While a-Si is more efficient in the blue part of the solar spectrum, and therefore spectra with low AM (high sun elevation angles  $\gamma_s$ ) are adequate, crystalline Si-technologies perform best in the red part of the solar spectrum and therefore high AM (low sun elevation angles  $\gamma_s$ ) are preferable. Fig. 2 shows the relative change of PV conversion efficiency vs. AM 1.5 at standard test conditions (STC).

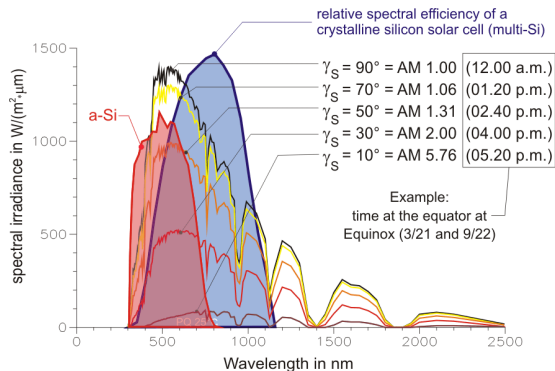


**Figure 1:** Spectral conversion efficiency of a-Si and multi-c-Si solar cells and their match to sun's spectra during a day, corresponding to sun's elevation angles  $\gamma_s$ .

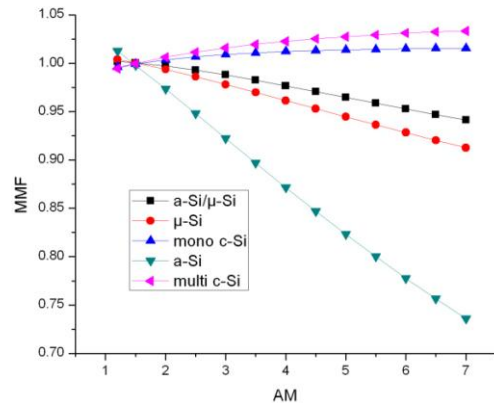


**Figure 2:** Relative change of conversion efficiency (MMF – mismatch factor) vs. STC (AM 1.5) calculated as a function of relative air mass (AM) for different PV technologies using standard spectra given by CIE 85 [6].

**2.2 Weak light performance**

Performance evaluation is even getting more complex due the change of conversion efficiency at different irradiance levels – the so-called “weak light performance”. For the different technologies this has been examined indoor via a solar flash simulator (Pasan IIIb) equipped with several neutral density filters (100, 200, 400, 800 W/m<sup>2</sup>) to change the irradiance level and also outdoor measurements. Results are shown in Fig. 3.

The better performance of  $\mu$ a-Si and in particular of a-Si for low a medium irradiance levels can be attributed to a relatively its high series resistance, so best performance cannot be achieved under STC. The deviation between the simulator results and the outdoor measurements in Fig. 3 can be explained by additional effects during outdoor measurements, such as spectral effects and changing angle of incidence. Outdoor data has been referenced via  $I_{sc}$  at STC to allow calculation of the actual irradiance.

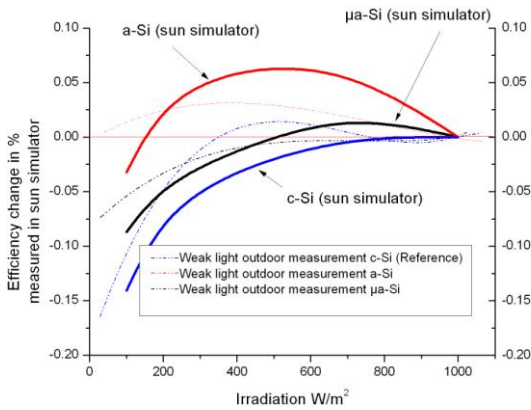


**Figure 3:** Comparing performance at different irradiance levels for different PV technologies (single junction a-Si and c-Si as well as tandem  $\mu$ -Si/a-Si). Data has been obtained via outdoor measurements and via sun simulator (Pasan IIIb, AM 1.5 plus neutral density filters).

While conversion efficiency is not constant for the range of irradiance levels occurring, the irradiance statistics of location becomes relevant (instead of just an average irradiance level). An example for irradiance statistics of some locations is given in Fig. 4.

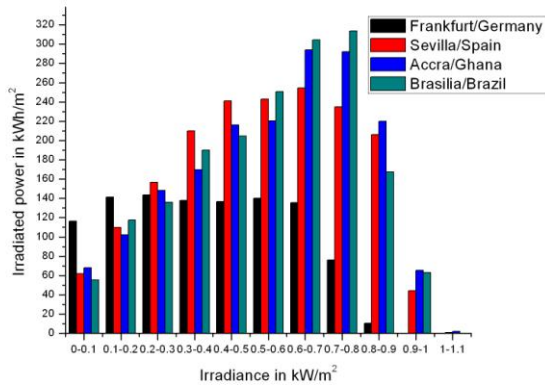


**Figure 4:** Statistics in terms of frequency distribution of global irradiance levels for different locations (module elevation angle  $\gamma_M = \text{latitude} - 20^\circ$ ).

## 2 MEASUREMENTS & RESULTS

### 2.1. Effect of Air Mass and Turbidity

In this chapter the two most important outdoor parameters for the spectral effect are examined: Air-Mass (AM) and turbidity (diffuse to global ratio of solar irradiance).

The data set has been recorded in Berlin, Germany during the period of 25<sup>th</sup> of February 2009 and 1<sup>st</sup> of March 2010. The module orientation was straight South; the module elevation angle was  $37^\circ$ . Only irradiance values above the threshold of  $100 \text{ W/m}^2$  have been recorded, also only data has been accepted which did show a deviation of less than 10% between Pyranometer (Schenk star-pyranometer) and Si-sensor irradiance measurement values.

The measured effects on  $I_{SC}$  (resp. power output) for different turbidity classes as a function of air mass are plotted in Fig. 5-7. It can be seen that for all turbidity levels performance of c-Si stays relatively constant, while a-Si and  $\mu$ -Si show a decrease of performance at increasing AM values – as expected. For high turbidity levels the spectrum becomes more bluish, thus increasing the performance of a-Si and  $\mu$ -Si.

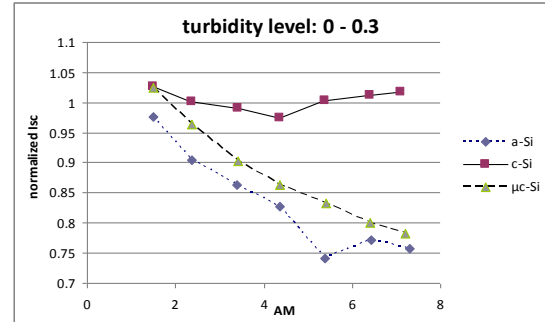


**Figure 5:** Performance comparison of c-Si,  $\mu$ -Si and a-Si cell technologies in terms of normalized and temperature-compensated short-circuit current ( $I_{SC}$ ) as a result of outdoor measurements during 2009 for diffuse sky in Berlin, Germany, as a function of relative Air Mass (AM).

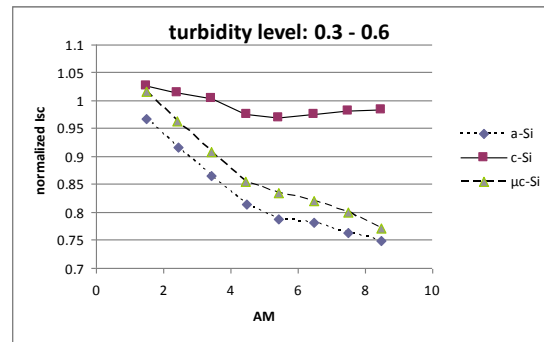


**Figure 6:** Performance comparison c-Si,  $\mu$ -Si and a-Si cell technologies in terms of normalized and temperature-compensated short-circuit current ( $I_{SC}$ ) as a result outdoor measurements during 2009 for intermediate turbidity in Berlin, Germany, as a function of relative Air Mass (AM).

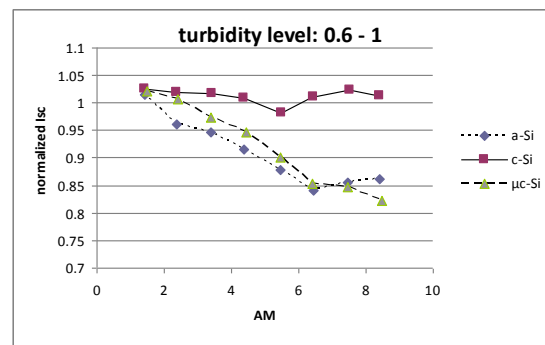


**Figure 7:** Performance comparison of c-Si,  $\mu$ -Si and a-Si cell technologies in terms of normalized and temperature-compensated short-circuit current ( $I_{SC}$ ) as a result outdoor measurements during 2009 for diffuse sky in Berlin, Germany, as a function of relative Air Mass (AM).

For temperature compensation of  $I_{SC}$  the temperature coefficients given in Table I have been applied.

**Table I:** Measured temperature coefficients for  $I_{SC}$

PV technology	$I_{SC}$ temperature coefficient
multi-c-Si	+ 0.05% /K
$\mu$ a-Si (tandem)	+ 0.0832% /K
a-Si (single junction)	+ 0.0942% /K

In order to examine the effect of turbidity more in detail and see both parameters (AM and turbidity) in a single graph, the data of Fig. 5-7 has been plotted as a 3D plot. The results are shown as a relative performance change in Fig. 8 for a-Si vs. c-Si and in Fig. 9 for  $\mu$ a-Si vs. c-Si.

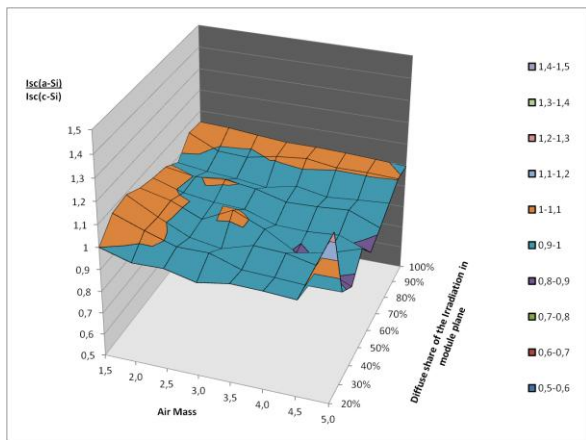


Fig. 8: Measured ratio of  $I_{sc}$  for a-Si vs. c-Si related to AM-values and diffuse/direct irradiance share (turbidity).

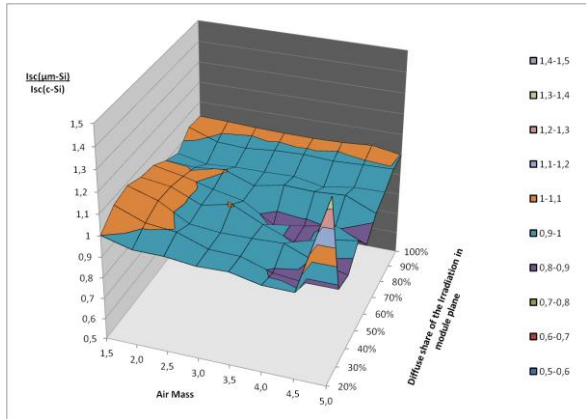


Fig. 9: Measured ratio of  $I_{sc}$  for  $\mu$ a-Si vs. c-Si related to AM-values and diffuse/direct irradiance share (turbidity).

### 2.2 Effect of degradation

The effect of air mass and turbidity on performance as described in chapter 2.1 is not constant during the whole year due to degradation effects of a-Si and  $\mu$ a-Si for low temperatures during the winter period and annealing effects for high temperatures during summer. This effect has been investigated in parallel to the measurements above; the results are shown in Fig. 10 for a-Si vs. c-Si and in Fig. 11 for  $\mu$ a-Si vs. c-Si.

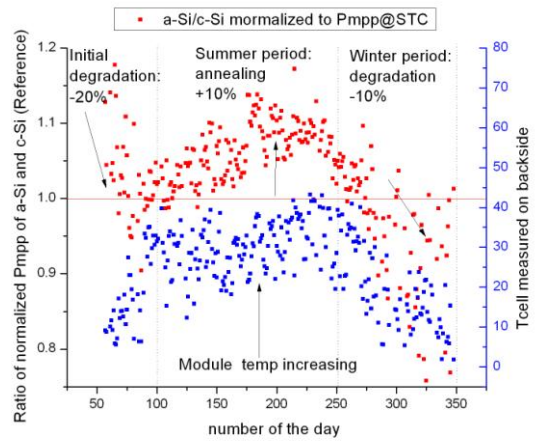


Fig. 10: Measured data of module temperature and relative performance change a-Si compared to c-Si. Data normalized to  $P_{mpp}$  at standard test conditions (STC), during one year (3/2009-2010) as a daily average.

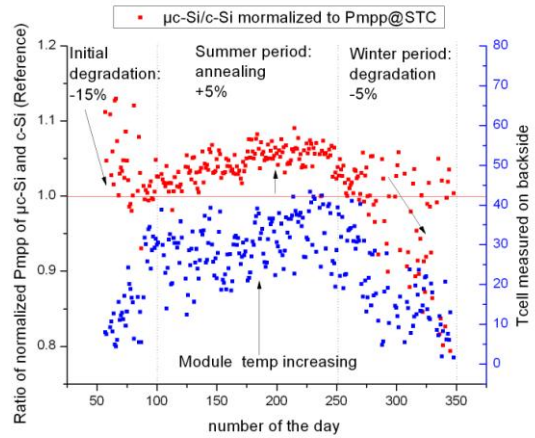


Fig. 11: Measured data of module temperature and relative performance change  $\mu$ a-Si compared to c-Si. Data normalized to  $P_{mpp}$  at standard test conditions (STC), during one year (3/2009-2010) as a daily average.

### 2.3 Energy yield

The most interesting result for the end-user is the comparison of the energy yields of the different PV technologies (including all effects described in chapter 2.1 and 2.2), this is given in Table II.

**Table II:** Relative electrical energy yield comparison of a-Si and  $\mu$ a-S thin film technologies vs. c-Si over one year (3/2009-2010) in Berlin, Germany

PV technology	relative electrical energy yield
multi-c-Si	1.000
$\mu$ a-Si (tandem)	1.023
a-Si (single junction)	1.020

For the local conditions in Berlin, Germany a slight advantage in the vicinity of 2% for the thin film technologies has been observed.

### 3 CONCLUSIONS

Amorphous silicon modules show higher energy yields compared to crystalline modules for diffuse light irradiation. This was as well calculated with the spectral mismatch given by the sky spectra in CIE 85 and the spectral response for single junction modules and detected from field measurements. Highly diffuse skies and high sun elevation angles result in the largest current increases for amorphous based modules over crystalline silicon modules. For moderate diffuse skies c-Si performs better. In total, a slight relative increase of 2% for a-Si and  $\mu$ -Si has been observed.

### 4 OUTLOOK

Other locations such as Rio de Janeiro, Brazil are under investigation. Further efforts are focusing on modeling the degradation and recovery cycles for tandem cells with the aim to clarify which combination of bottom and top cell offer optimal power output for initial and degraded conditions, as well as optimized spectral mismatch factors for real sky spectra under field conditions.

### 5 LITERATURE

[1] Krauter, S., Preiss, A., Ferretti, N. and P. Grunow: "PV yield prediction for thin film technologies and the effect of input parameters inaccuracies" 23<sup>rd</sup> European Photovoltaic Solar Energy Conference and Exhibition, Valencia (Spain), September, 1–5, 2008, p. 740-743.

[2] Grunow, P., Preiss, A., Koch, S. and S. Krauter. Koch: "Yield and Spectral Effects of a-Si Modules." Proceedings of the 24<sup>th</sup> European Photovoltaic Solar Energy Conference and Exhibition, Hamburg (Germany), September, 21–25 2009, pp. 2846-2849.

[3] R. Gottschalg et al., "Effect of spectral mismatch on power rating measurements – a comparison of indoor and outdoor measurements for single and multi-junction devices" 22nd PVSEC, Milano (2007), p. 2621.

[4] T. Minemoto et al., "Difference in the outdoor performance of bulk and thin-film silicon-based photovoltaic modules", Solar energy Materials & Solar Cells 93 (2009), p. 1062.

[5] Martín N, Ruiz J.M, "A new model for PV modules angular losses under field conditions", International Journal of Solar Energy 2002: 22(1); pp. 19-31.

[6] CIE 85-1989, Solar Spectrum Irradiance ISBN 3 900 734 22 4, Table 7 & 8.